



# Methane sulfonic acid enhanced formation of molecular clusters of sulfuric acid and dimethyl amine

University of Helsinki, Department of Physics, Division of Atmospheric Sciences, P.O. Box 64, 00014 Helsinki, Finland  
University of Copenhagen, Department of Chemistry, Universitetsparken 5, 2100, Copenhagen, Denmark

Correspondence to: N. Bork (nicolai.bork@helsinki.fi)

**Abstract.** Over oceans and in coastal regions methane sulfonic acid (MSA) is present in substantial concentrations in aerosols and in the gas phase. We present an investigation of the effect of MSA on sulfuric acid and dimethyl amine (DMA) based cluster formation rates. From systematic conformational scans and well tested ab initio methods, we optimize structures of all  $\text{MSA}_x(\text{H}_2\text{SO}_4)_y\text{DMA}_z$  clusters where  $x + y \leq 3$  and  $z \leq 2$ . The resulting thermodynamic data is used in the Atmospheric Cluster Dynamics Code and the effect of MSA is evaluated by comparing ternary MSA- $\text{H}_2\text{SO}_4$ -DMA cluster formation rates to binary  $\text{H}_2\text{SO}_4$ -DMA cluster formation rates. Within the range of atmospherically relevant MSA concentrations, we find that MSA may increase cluster formation rates by up to one order of magnitude, although typically, the increase will be less than 300 % at 258 K, less than 100 % at 278 K and less than 15 % at 298 K. The results are rationalized by a detailed analysis of the the main growth paths of the clusters. We find that MSA enhanced clustering involves clusters containing one MSA molecule, while clusters containing more than one MSA molecule do not contribute significantly to the growth.

The decisive importance of sulfuric acid for atmospheric aerosol formation is well established, but within the last decades it has become evident that at least one, but probably more stabilizing species participate as well (Weber et al., 1996; Almeida et al., 2013). Nitrogenous bases, most efficiently dimethyl amine (DMA), and highly oxidized organic compounds are known to enhance sulfuric acid based aerosol formation. However, in locations where these are sparse other species may contribute significantly.

Methane sulfonic acid (MSA) is the simplest organosulfate and is a well known oxidation product of dimethylsulfide. Over oceans and in coastal regions, gaseous MSA is present in concentrations of about 10 to 50 % of the gaseous sulfuric acid ( $\text{H}_2\text{SO}_4$ ) concentration, (Berresheim et al., 2002; Huebert et al., 1996) although MSA/ $\text{H}_2\text{SO}_4$  ratios up to 250 % have been reported (Davis et al., 1998). Similarly, in sub- $\mu\text{m}$  aerosol particles MSA is typically found in concentrations of 5 to 30 % of the sulfate concentrations (Ayers et al., 1991; Huebert et al., 1996; Kerminen et al., 1997) although MSA/sulfate ratios around 100 % have been reported in aerosols smaller than 0.2  $\mu\text{m}$  (Facchini et al., 2008). It is generally accepted that much particulate MSA originate from surface oxidation of dimethyl sulfoxide (DMSO) and methane sulfinic acid (MSIA) (Davis et al., 1998; Barnes et al., 2006). However, in a recent study by Dall'Osto et al. (2012), gaseous MSA concentrations were found to decrease during marine particle formation events, suggesting that MSA may contribute to growth and possibly formation of the initial molecular clusters seeding aerosol formation.

Several laboratory and theoretical studies have attempted to explain these observations and determine at which state MSA enters the aerosol particle. Earlier studies have often used classical nucleation theory to predict or reproduce particle formation rates of various mixtures of  $\text{H}_2\text{SO}_4$ , MSA and water, generally finding that MSA is of minor importance

## 1 Introduction

One of the least understood micro-physical processes in the atmosphere is the conversion of low volatile gaseous molecules into an aerosol particle. Aerosol particles are a major source of cloud condensation nuclei and aerosol formation represents one of the largest uncertainties in climate and cloud models (Solomon et al., 2007; Kazil et al., 2010; Pierce and Adams, 2009). Despite recent advances in theory and instrumentation, the chemical composition of the molecular clusters forming the seeds for the thermally stable aerosol particles remains highly uncertain in most locations.

(Wyslouzil et al., 1991; Napari et al., 2002; Van Dingenen and Raes, 1993). Later studies by Dawson et al. (2012) and Bzdek et al. (2011) combining flow tube experiments and ab initio calculations, found that water and nitrogenous bases enhanced MSA based aerosol formation and that amines are more efficient than ammonia, and recently, Dawson et al. (2014) found that trimethylamine was susceptible for substitution by both methylamine and DMA. Further, Dall'Osto et al. (2012) used quantum chemical calculations, considering the molecular clusters containing up to two acids and one DMA molecule, to support the hypothesis that MSA, H<sub>2</sub>SO<sub>4</sub> and DMA could co-exist in newly formed molecular clusters.

These studies have prompted a more rigorous ab initio based evaluation of whether MSA contributes to aerosol formation or mainly enters the aerosol during growth. This study targets the enhancing effect of MSA on sulfuric acid-DMA based cluster formation. Via systematic conformational searches we have obtained minimum free energy structures of clusters of composition MSA<sub>x</sub>(H<sub>2</sub>SO<sub>4</sub>)<sub>y</sub>DMA<sub>z</sub> where  $x + y \leq 3$  and  $z \leq 2$ . The corresponding thermodynamic data is used in the Atmospheric Cluster Dynamics Code (ACDC) (McGrath et al., 2012; Olenius et al., 2013) whereby the enhancing effect of MSA is obtained by comparing ternary MSA-H<sub>2</sub>SO<sub>4</sub>-DMA to binary H<sub>2</sub>SO<sub>4</sub>-DMA based cluster formation rates.

The clusters studied in this work do not contain water molecules due to the considerable additional computational effort required to obtain the necessary thermodynamic data. Hydration can be expected to stabilize weakly bound clusters more than strongly bound clusters and it is therefore conceivable that we will underestimate the contribution from some of the minor growth pathways. However, since DMA is a much stronger base than water, hydration is not likely to have a significant effect on the stability of clusters containing DMA. Therefore, the main growth pathways and growth rates are unlikely to change significantly due to hydration. See e.g. Almeida et al. (2013) and Henschel et al. (2014) for further discussion.

## 2 Computational details

### 2.1 Ab initio calculations

The most critical parameters in cluster growth models are the cluster binding free energies since the evaporation rate depends exponentially on these. At present, density functional theory (DFT) and second order Møller-Plesset perturbation theory (MP2) are the most popular ab initio methods for calculating the thermodynamics of molecular clusters. It is often mentioned that average uncertainties are on the order of 1 kcal mol<sup>-1</sup>, but depending on the specific system and method, uncertainties may be significantly larger. Therefore, careful testing and validation should precede each study, which we will discuss in the following.

Since acid-base clustering is considered one of the fundamental processes driving aerosol formation, we have tested the performance of four commonly used DFT functionals and MP2, comparing these to previously published data. Also, the effect of electronic energy corrections from high level coupled cluster calculations is tested. The basis set effects have previously been found to be much less significant, provided that a basis set of at least triple- $\zeta$  quality is used (Bork et al., 2014a). In this study we use the 6-311++G(3df,3pd) (Francl et al., 1982; Clark et al., 1983) basis set in all DFT and MP2 calculations.

From the first and second sections of Table 1, we see that the CCSD(T)-F12/VDZ-F12 electronic energy corrections significantly reduce the scatter of the data. This suggests that the thermal and zero-point vibrational terms are well produced by the four DFT functional and MP2, and that the main errors are associated with the electronic energies. Also, the data reveal that amongst the tested methods the M06-2X,  $\omega$ B97X-D and PW91 density functionals perform well whereas B3LYP performs poorly on systems representative by clustering of H<sub>2</sub>SO<sub>4</sub> and MSA with DMA.

In several recent studies (Bork et al., 2014a,b; Leverentz et al., 2013; Elm et al., 2012, 2013b) the M06-2X functional (Zhao and Truhlar, 2008) has been shown to be amongst the most reliable and accurate density functionals with respect to binding free energies of molecular clusters. Therefore, its performance for the present systems was investigated in greater detail. Table 2 shows the effect of a CCSD(T)-F12a/VDZ-F12 single point electronic energy correction to the M06-2X Gibbs free energy for six relevant reactions. For the formation of the DMA · H<sub>2</sub>SO<sub>4</sub> and DMA · MSA complexes a slight underestimation is observed in agreement with previous studies of similar systems (Bork et al., 2014a; Elm et al., 2012, 2013b). For the MSA · H<sub>2</sub>SO<sub>4</sub>, (H<sub>2</sub>SO<sub>4</sub>)<sub>2</sub> and MSA<sub>2</sub> complexes the DFT values are seen to overestimate the Gibbs free energies of formation by up to 2.14 kcal mol<sup>-1</sup>. No reliable representative experimental data exist for comparison of acid-acid cluster binding energies. However, the binding energy of (H<sub>2</sub>SO<sub>4</sub>)<sub>2</sub> has been investigated by Ortega et al. (2012), using MP2 up to pentuple  $\zeta$  basis sets including also anharmonic and relativistic effects, arriving at a value of -7.91 kcal mol<sup>-1</sup>. This indicates that the apparent overbinding of the M06-2X functional is less severe than 2 kcal mol<sup>-1</sup> and that M06-2X based errors in binding energies of molecular clusters with both acid-acid and acid-base bonds will tend to cancel out rather than to accumulate.

All DFT and MP2 geometry optimizations and frequency calculations are performed using Gaussian 09 (Revision B.01, <http://www.gaussian.com>) and all CCSD(T)-F12 calculations are performed using Molpro (Version 2012.1, <http://www.molpro.net>).

Besides an appropriate computational method, a second pre-requisite for obtaining correct cluster binding free energies is to obtain the global minimum energy structures. In

this study we employ a systematic sampling technique initiated by 1000 auto generated guess structures, pre-optimized using the PM6 semi-empirical method (Stewart, 2007). The up to 100 best guess structures are further refined using M06-2X/6-311++G(3df,3pd). For full detail of the sampling technique we refer to our previous investigations (Elm et al., 2013c,a). Additionally, guess structures for all cluster compositions were manually constructed based on previously published (H<sub>2</sub>SO<sub>4</sub>)<sub>x</sub>DMA<sub>y</sub> and (H<sub>2</sub>SO<sub>4</sub>)<sub>x</sub>(NH<sub>3</sub>)<sub>y</sub> structures (Nadykto et al., 2011; Ortega et al., 2012). In several cases this lead to identical structures as the above mentioned systematic sampling, but in no cases did the manual approach lead to improved binding energies compared to the systematic approach.

## 2.2 Cluster growth model

The resulting thermodynamic data was studied with the kinetic model Atmospheric Cluster Dynamics Code (ACDC) (McGrath et al., 2012; Olenius et al., 2013). The code solves the time evolution of molecular cluster concentrations for a given set of clusters and ambient conditions, considering all possible collision and fragmentation processes. In this study, ACDC is used to find the steady-state of the cluster distribution at given concentrations of MSA, H<sub>2</sub>SO<sub>4</sub> and DMA. The collision rate coefficients are calculated as hard-sphere collision rates and the evaporation rate coefficients are calculated from the Gibbs free energies of formation according to detailed balance.

As the vapour-phase concentrations of MSA and H<sub>2</sub>SO<sub>4</sub> generally are measured with chemical ionization mass spectrometry (CIMS), the atmospheric concentrations reported in the literature are likely to include contributions from acid molecules clustered with bases, in addition to the bare acid monomer (Kupiainen-Määttä et al., 2013). Therefore the acid concentrations in ACDC (both MSA and H<sub>2</sub>SO<sub>4</sub>) are defined as the sum of all clusters consisting of one acid molecule and any number of DMA molecules. An external sink with a loss rate coefficient of  $2.6 \times 10^{-3} \text{ s}^{-1}$ , corresponding to coagulation onto pre-existing larger particles is used for all clusters (Dal Maso et al., 2008). Testing showed that variations in this value between  $10^{-3} \text{ s}^{-1}$  and  $5 \times 10^{-3} \text{ s}^{-1}$  did not affect the main conclusions of this study (Figure S1).

When a collision leads to a cluster that is larger than the simulated system, the cluster is allowed to grow out if it contains at least three acid and three base molecules since these compositions are assumed to be along the main growth path. The probability of a three acid-three base cluster to grow further vs. to re-evaporate back into the system was investigated by optimizing also the MSA(H<sub>2</sub>SO<sub>4</sub>)<sub>2</sub>DMA<sub>3</sub> cluster. At  $T = 298 \text{ K}$ , for example, the reaction



has  $\Delta G_{298\text{K}}^\circ = 14.5 \text{ kcal mol}^{-1}$  corresponding to an evaporation rate of  $4.3 \times 10^{-1} \text{ s}^{-1}$  which can be

compared to a collision rate with another DMA or H<sub>2</sub>SO<sub>4</sub> molecule of  $8.4 \times 10^{-2} \text{ s}^{-1}$  or  $5.7 \times 10^{-4} \text{ s}^{-1}$ , respectively ( $[\text{DMA}] = 10^8 \text{ molecules cm}^{-3}$  and  $[\text{H}_2\text{SO}_4] = 10^6 \text{ molecules cm}^{-3}$ ). At  $T = 258 \text{ K}$ ,  $\Delta G_{258\text{K}}^\circ = 16.1 \text{ kcal mol}^{-1}$  and the evaporation rate of  $4.4 \times 10^{-4} \text{ s}^{-1}$  is much lower compared to collision rates with DMA or H<sub>2</sub>SO<sub>4</sub> of  $7.8 \times 10^{-2} \text{ s}^{-1}$  or  $5.3 \times 10^{-4} \text{ s}^{-1}$ . This reveals that, depending on the conditions, evaporation of 3 acid and 3 based clusters can be significant and that larger clusters than considered in this study should be included for quantitative assessments of formation rates of nanometer sized MSA-H<sub>2</sub>SO<sub>4</sub>-DMA based particles, in particular at higher temperatures. Our analysis is therefore restricted to formation rates of 3 acid-3 base molecular clusters.

Cluster types outside the simulation box not containing at least three acids and at least three base molecules are considered unstable and hence much more likely to shrink by evaporations rather than being stabilized by another collision. Therefore these types of clusters are brought back into the simulation by monomer evaporations. In the case that the evaporating molecules are excess acid, the first evaporating molecule is assumed to be MSA since it is a weaker acid than H<sub>2</sub>SO<sub>4</sub>. From these simulations we determine the formation rate of clusters that grow out of the system, and track the main growth routes by following the flux through the system (Olenius et al., 2013).

## 3 Results

### 3.1 Structures and thermodynamics

Structures and thermodynamic data for all of the most stable MSA<sub>x</sub>(H<sub>2</sub>SO<sub>4</sub>)<sub>y</sub>DMA<sub>z</sub> clusters, where  $x + y \leq 3$  and  $z \leq 2$ , are given as Supplement. These clusters share several structural features. In all cases where the number of base molecules does not exceed the number of acid molecules (MSA or H<sub>2</sub>SO<sub>4</sub>) the DMA moiety is protonated but in none of the clusters SO<sub>4</sub><sup>2-</sup> is found. In most clusters containing both H<sub>2</sub>SO<sub>4</sub> and MSA, H<sub>2</sub>SO<sub>4</sub> is more acidic than MSA. However, in a few cases including the most stable H<sub>2</sub>SO<sub>4</sub> · MSA · DMA cluster, deprotonated MSA and doubly protonated H<sub>2</sub>SO<sub>4</sub> is seen in the same cluster (Fig. 1a). This is in accordance with the findings of Dall'Osto et al. (2012). Another common feature is the monolayer-like rather than bulk-like structures of even the largest clusters investigated, e.g. MSA(H<sub>2</sub>SO<sub>4</sub>)<sub>2</sub>DMA<sub>3</sub> (Fig. 1b). This tendency has been seen in other studies of similar systems, e.g. H<sub>2</sub>SO<sub>4</sub>-DMA based clusters (Ortega et al., 2012) and HSO<sub>4</sub><sup>-</sup>-H<sub>2</sub>SO<sub>4</sub>-NH<sub>3</sub> based clusters (Herb et al., 2012). This is opposite to clusters containing several water molecules where bulk-like H<sub>2</sub>O structures tend to be more stable (Bork et al., 2013, 2011).

It is well known that strong acids and strong bases tend to form strong hydrogen bonds and more stable clus-

ters than weaker acids and bases. Since MSA is a weaker acid than H<sub>2</sub>SO<sub>4</sub> it is expected that the MSA · DMA binding energy is weaker than the H<sub>2</sub>SO<sub>4</sub> · DMA binding energy (Table 2). It is, on the other hand, surprising that the MSA · H<sub>2</sub>SO<sub>4</sub> bond is at least 1.5 kcal mol<sup>-1</sup> stronger than the H<sub>2</sub>SO<sub>4</sub> · H<sub>2</sub>SO<sub>4</sub> bond, and that the MSA · MSA bond is at least 0.5 kcal mol<sup>-1</sup> stronger than the H<sub>2</sub>SO<sub>4</sub> · H<sub>2</sub>SO<sub>4</sub> bond. In larger clusters, H<sub>2</sub>SO<sub>4</sub> is, however, significantly more stabilized compared to MSA, and, besides the MSA dimer, clusters containing more than one MSA molecule are less stable than their corresponding H<sub>2</sub>SO<sub>4</sub> containing analogues (Table S1).

### 3.2 Clustering enhancements

To analyse the clustering abilities of MSA, a series of ACDC simulations based on these thermodynamics were performed at varying conditions. As a first measure, the binary cluster formation rate of MSA and DMA was compared to those of H<sub>2</sub>SO<sub>4</sub> and DMA at similar conditions, i.e. the ratio

$$r_1 = \frac{J([\text{H}_2\text{SO}_4]=0, [\text{MSA}]=x, [\text{DMA}]=y)}{J([\text{H}_2\text{SO}_4]=x, [\text{MSA}]=0, [\text{DMA}]=y)} \quad (1)$$

where  $J$  denotes the cluster formation rate at the indicated conditions.

This was calculated for three temperatures (258, 278 and 298 K) spanning the boundary layer to the lower half of the troposphere, and  $x$  in the range from  $10^5$  to  $2 \times 10^6$  molecules cm<sup>-3</sup>, corresponding to typical H<sub>2</sub>SO<sub>4</sub> and MSA concentrations as described in the introduction. We used three DMA concentrations spanning most reported marine values ( $y = 10^7$ ,  $10^8$  and  $10^9$  molecules cm<sup>-3</sup>) (see Gibb et al., 1999 and Table 4 in Ge et al., 2011). Only field data from the boundary layer is available and the results presented here may thus not be representative for the free troposphere, if DMA concentrations turn out to be very different from the boundary layer. The resulting values for  $r_1$  are shown in Fig. S2. In all cases, we find that this ratio is less than  $10^{-2}$  and, as expected, we conclude that binary MSA and DMA based cluster formation is of minor importance under normal conditions.

The main objectives of this study is to investigate the errors of neglecting MSA as a source of condensable vapour, as this is the case in most present aerosol formation parametrizations and models. A suitable measure for this is the ratio

$$r_2 = \frac{J([\text{H}_2\text{SO}_4]=10^6, [\text{MSA}]=x, [\text{DMA}]=y)}{J([\text{H}_2\text{SO}_4]=10^6, [\text{MSA}]=0, [\text{DMA}]=y)} \quad (2)$$

where  $J$  denotes the cluster formation rate at the indicated MSA concentration on top of a representative H<sub>2</sub>SO<sub>4</sub> concentration, here chosen to be  $10^6$  molecules cm<sup>-3</sup>. All other parameters are as defined above.  $r_2$  is shown in Fig. 2 as a function of [MSA].

As expected both temperature and DMA concentrations are important parameters for the ratio,  $r_2$ . At lower temperatures, entropy effects are decreased and all binding free energies are more negative. In this case, the cluster growth becomes increasingly insensitive to the chemical nature of the colliding species and more dependent on the collision frequency. At high DMA levels, DMA is in large excess compared to H<sub>2</sub>SO<sub>4</sub> and cluster growth is thus limited by acid collisions. In this case, having an extra source of acid has a larger effect than at lower DMA concentrations where the DMA excess is less severe. The approximately linear dependence of  $r_2$  on the MSA concentration could indicate that only a single MSA molecule participates at these cluster sizes. This will be further investigated in Sect. 3.3.

Adding a small amount of MSA has a small effect on the cluster formation rate, but in locations where approximately equimolar amounts of MSA and H<sub>2</sub>SO<sub>4</sub> are present, this added MSA increases the cluster formation rate by ca. 15 % at 298 K, by ca. 100 % at 278 K, but by more than 300 % at 258 K in the case of [DMA]= $10^9$  molecules cm<sup>-3</sup>. Recalling the discussion in the Sect. 2.1, and taking the latter case as example, this increase may, however, be as small 200 % or as large as 500 % if the binding energies are 1 kcal mol<sup>-1</sup> over- or underestimated, respectively (Fig. S3).

We consider a final descriptive ratio, indicating the effects of an unknown concentration of MSA compared to a similar deficiency in the H<sub>2</sub>SO<sub>4</sub> concentration. This is given as the ratio

$$r_3 = \frac{J([\text{H}_2\text{SO}_4]=10^6, [\text{MSA}]=x, [\text{DMA}]=y)}{J([\text{H}_2\text{SO}_4]=10^6 + x, [\text{MSA}]=0, [\text{DMA}]=y)} \quad (3)$$

where  $J$  represents the cluster formation rate at the given conditions and  $x$  represents the added/deficient concentration of MSA or H<sub>2</sub>SO<sub>4</sub> in addition to a fixed H<sub>2</sub>SO<sub>4</sub> concentration, again chosen to be  $10^6$  molecules cm<sup>-3</sup>. This ratio is shown in Fig. 3 for  $T = 258$  K as function of  $x$  with the same conditions as above. This figure confirms that MSA is a less efficient clustering agent than H<sub>2</sub>SO<sub>4</sub>, but also that the difference is very concentration dependent. Adding a small extra amount of acid, e.g. up to  $2 \times 10^5$  molecules cm<sup>-3</sup>, MSA is ca. 60–90 % as efficient as a similar amount of added H<sub>2</sub>SO<sub>4</sub>. However, when the acid concentrations is doubled from the [H<sub>2</sub>SO<sub>4</sub>]= $10^6$  molecules cm<sup>-3</sup> forming the reference conditions, the added MSA yields an increased cluster formation rate of ca. 20–60 % compared to the same amount of added H<sub>2</sub>SO<sub>4</sub>. When the acid concentration is tripled the enhancement is ca. 10–40 %. See Figs. S4 and S5 for corresponding plots of  $T = 278$  K and  $T = 298$  K.

### 3.3 Growth paths

The ACDC model was used to track the main growth pathways of the clusters growing out of the simulation system. As shown in Fig. 4, the flux through the system proceeds principally via two clustering mechanisms: one that involves pure

H<sub>2</sub>SO<sub>4</sub>-DMA clusters, and another one where the clusters contain one MSA molecule in addition to H<sub>2</sub>SO<sub>4</sub> and DMA. Clusters containing more than one MSA molecule were not found to contribute significantly to the growth. The relative contribution of the two growth mechanisms to the flux out of the system depends on the concentrations of the different species; at a higher MSA concentration the contribution of MSA-containing clusters is more prominent, as can be expected. In the case of [DMA]=10<sup>8</sup> molecules cm<sup>-3</sup> between 11 and ca. 51 % of the clusters growing out of the simulation box contains one MSA at [MSA]=10<sup>5</sup> molecules cm<sup>-3</sup> and 10<sup>6</sup> molecules cm<sup>-3</sup> (Fig. 4). Since such clusters contain three acid molecules (H<sub>2</sub>SO<sub>4</sub> or MSA), this implies overall MSA/H<sub>2</sub>SO<sub>4</sub> ratios of 3 % and 17 % at these conditions.

The growth of pure H<sub>2</sub>SO<sub>4</sub>-DMA clusters begins with the formation of the H<sub>2</sub>SO<sub>4</sub>·DMA heterodimer, whereas the first step on the MSA-H<sub>2</sub>SO<sub>4</sub>-DMA growth route is the MSA·H<sub>2</sub>SO<sub>4</sub> complex or the MSA·H<sub>2</sub>SO<sub>4</sub>·DMA cluster, formed by collision of MSA and H<sub>2</sub>SO<sub>4</sub>·DMA. This is understandable as H<sub>2</sub>SO<sub>4</sub>·DMA and MSA·H<sub>2</sub>SO<sub>4</sub> are the two most stable dimers that can form in the system (Table 2). After the formation of the initial complex, the growth proceeds through subsequent collisions with H<sub>2</sub>SO<sub>4</sub> and DMA molecules, but also H<sub>2</sub>SO<sub>4</sub>·DMA dimers that are bound strongly enough to exist in notable amounts. In the MSA-H<sub>2</sub>SO<sub>4</sub>-DMA system, the H<sub>2</sub>SO<sub>4</sub>·DMA dimers contribute up to approximately 15 % of the H<sub>2</sub>SO<sub>4</sub> concentration measurable by CIMS (i.e. clusters consisting of one H<sub>2</sub>SO<sub>4</sub> and zero or more DMA molecules) in the conditions of Fig. 4, whereas MSA·DMA dimer concentrations, on the other hand, are negligible.

## 4 Conclusions

Methane sulfonic acid (MSA) is found in considerable quantities in the gas and aerosol phase over oceans and in coastal regions. We have investigated the effect and role of MSA in formation of molecular clusters in atmospheres containing various quantities of MSA, H<sub>2</sub>SO<sub>4</sub> and dimethyl amine (DMA). We use the kinetic model Atmospheric Cluster Dynamics Code and quantum chemical calculations of clusters containing up to three acids (MSA and/or H<sub>2</sub>SO<sub>4</sub>) and two DMA molecules.

In accordance with numerous previous studies, we confirm that MSA is a less potent clustering agent than H<sub>2</sub>SO<sub>4</sub>, but far from negligible at normal conditions. The effect of MSA depends on both temperature and concentrations of MSA and DMA, but we find that enhancements of binary H<sub>2</sub>SO<sub>4</sub>-DMA based cluster formation between 15 and 300 % are typical in the marine lower to mid-troposphere.

We analyse these findings by tracking the main growth paths. We find that at most a single MSA is present in the growing clusters at the conditions investigated here and, typically, MSA/H<sub>2</sub>SO<sub>4</sub> ratios are below ca. 15 % at these clus-

ter sizes. Using this model, we are thus unable to explain MSA/H<sub>2</sub>SO<sub>4</sub> ratios up to 30 % observed by Ayers et al. (1991), Huebert et al. (1996) and Kerminen et al. (1997) in small aerosol particles. This strengthens the hypotheses that surface oxidation of DMSO or MSIA is the major source of particulate MSA (Davis et al., 1998; Barnes et al., 2006). However, we have shown that MSA may enter the aerosol particle at the earliest possible stage and significantly assists in cluster formation.

This is a consequence of MSA being a strong acid, binding strongly to DMA and H<sub>2</sub>SO<sub>4</sub>, and that DMA in most pristine oceanic locations is in large excess compared to acid. For actual predictions of nanometer sized aerosol formation rates, larger clusters than the three acid-two base clusters studied here must be included in the kinetic model.

**Supplementary material related to this article is available online at:** <http://www.atmospheric-chemistry.net/journalurl/@pvol/@fpage/@pyear/@journalnameshortlower/@pvol/@fpage/@pyear-supplement.pdf>.

**Acknowledgements.** We thank Theo Kurtén for valuable suggestions and references. We thank the European Research Council (project 257360-MOCAPAF), the Academy of Finland Center of Excellence (project 272041) and the Villum Foundation for funding. We thank CSC Centre for Scientific Computing (Finland) and DCSC Danish Centre for Scientific Computing for computational resources.

## References

- references
- Almeida, J., Schobesberger, S., Kürten, A., et al.: Molecular understanding of sulphuric acid-amine particle nucleation in the atmosphere, *Nature*, 502, 359–363, 2013.
- Ayers, G., Ivey, J., and Gillett, R.: Coherence between seasonal cycles of dimethyl sulphide, methanesulphonate and sulphate in marine air, *Nature*, 349, 404–406, 1991.
- Barnes, I., Hjorth, J., and Mihalopoulos, N.: Dimethyl Sulfide and Dimethyl Sulfoxide and Their Oxidation in the Atmosphere, *Chem. Rev.*, 106, 940–975, 2006.
- Berresheim, H., Elste, T., Tremmel, H. G., Allen, A. G., Hansson, H.-C., Rosman, K., Dal Maso, M., Mäkelä, J. M., Kulmala, M., and O'Dowd, C. D.: Gas-aerosol relationships of H<sub>2</sub>SO<sub>4</sub>, MSA, and OH: observations in the coastal marine boundary layer at Mace Head, Ireland, *J. Geophys. Res.*, 107, 8100, doi:10.1029/2000JD000229, 2002.
- Bork, N., Kurtén, T., Enghoff, M. B., Pedersen, J. O. P., Mikkelsen, K. V., and Svensmark, H.: Ab initio studies of O<sub>2</sub><sup>-</sup>(H<sub>2</sub>O)<sub>n</sub> and O<sub>3</sub><sup>-</sup>(H<sub>2</sub>O)<sub>n</sub> anionic molecular clusters, *n* ≤ 12, *Atmos. Chem. Phys.*, 11, 7133–7142,

- doi:<http://dx.doi.org/10.5194/acp-11-7133-2011>, 2011.
- 485 Bork, N., Loukonen, V., and Vehkamäki, H.: Reactions and reaction rate of atmospheric SO<sub>2</sub> and O<sub>3</sub><sup>-</sup> (H<sub>2</sub>O)<sub>n</sub> collisions via molec- 545 ular dynamics simulations, *J. Phys. Chem. A*, 117, 3143–3148, 2013.
- 490 Bork, N., Du, L., and Kjaergaard, H. G.: Identification and characterization of the HCl-DMS gas phase molecular complex via infrared spectroscopy and electronic struc- 550 ture calculations, *J. Phys. Chem. A*, 118, 1384–1389, doi:<http://dx.doi.org/10.1021/jp411567x>, 2014.
- 495 Bork, N., Du, L., Reiman, H., Kurtén, T. and Kjaergaard, H. G.: Benchmarking Ab Initio Binding Ener- 555 gies of Hydrogen-Bonded Molecular Clusters Based on FTIR Spectroscopy, *J. Phys. Chem. A*, 118, 53165322, doi:<http://dx.doi.org/10.1021/jp5037537>, 2014.
- 500 Bzdek, B. R., Ridge, D. P., and Johnston, M. V.: Re- 560 activity of methanesulfonic acid salt clusters relevant to marine air, *J. Geophys. Res.-Atmos.*, 116, D03301, doi:<http://dx.doi.org/10.1029/2010JD015217>, 2011.
- 505 Clark, T., Chandrasekhar, J., Spitznagel, G. W., and 565 Schleyer, P. V. R.: Efficient diffuse function-augmented basis sets for anion calculations. III. The 3-21+G basis set for first-row elements, Li–F, *J. Comput. Chem.*, 4, 294–301, 1983.
- 510 Dal Maso, M., Hyvärinen, A., Komppula, M., Tunved, P., Kerminen, V., Lihavainen, H., Viisanen, Y., Hansson, H.-C., and 570 Kulmala, M.: Annual and interannual variation in boreal forest aerosol particle number and volume concentration and their connection to particle formation, *Tellus B*, 60, 495–508, 2008.
- 515 Dall’Osto, M., Ceburnis, D., Monahan, C., Worsnop, D. R., Bialek, J., Kulmala, M., Kurtén, T., Ehn, M., Wenger, J., 575 Sodeau, J., Healy, R., and O’Dowd, C.: Nitrogenated and aliphatic organic vapors as possible drivers for marine secondary organic aerosol growth, *J. Geophys. Res.-Atmos.*, 117, D12311, doi:10.1029/2012JD017522, 2012.
- 520 Davis, D., Chen, G., Kasibhatla, P., Jefferson, A., Tanner, D., 580 Eisele, F., Lenschow, D., Neff, W., and Berresheim, H.: DMS oxidation in the Antarctic marine boundary layer: comparison of model simulations and held observations of DMS, DMSO, DMSO<sub>2</sub>, H<sub>2</sub>SO<sub>4</sub> (g), MSA (g), and MSA (p), *J. Geophys. Res.-Atmos.*, 103, 1657–1678, 1998.
- 525 Dawson, M. L., Varner, M. E., Perraud, V., Ezell, M. J., Gerber, R. B., and Finlayson-Pitts, B. J.: Simplified mechanism for new particle formation from methanesulfonic acid, amines, and water via experiments and ab initio calculations, *P. Natl. Acad. Sci. USA*, 109, 18719–18724, 2012.
- 530 Dawson, M. L., Varner, M. E., Perraud, V., Ezell, M. J., Wilson, J., Zellenyuk, A., Gerber, R. B., and Finlayson-Pitts, B. J.: AmineAmine Exchange in AminiumMethanesulfonate Aerosols, *J. Phys. Chem. C*, DOI: 10.1021/jp506560w
- 535 Elm, J., Bilde, M., and Mikkelsen, K. V.: Assessment of density 595 functional theory in predicting structures and free energies of reaction of atmospheric prenucleation clusters, *J. Chem. Theory Comput.*, 8, 2071–2077, 2012.
- 540 Elm, J., Bilde, M., and Mikkelsen, K. V.: Influence of nucleation precursors on the reaction kinetics of methanol with the OH rad- 600 ical, *J. Phys. Chem. A*, 117, 6695–6701, 2013a.
- Elm, J., Bilde, M., and Mikkelsen, K. V.: Assessment of binding energies of atmospherically relevant clusters, *Phys. Chem. Chem. Phys.*, 15, 16442–16445, 2013b.
- Elm, J., Fard, M., Bilde, M., and Mikkelsen, K. V.: Interaction of glycine with common atmospheric nucleation precursors, *J. Phys. Chem. A*, 117, 12990–12997, 2013c.
- Facchini, M. C., Decesari, S., Rinaldi, M., Carbone, C., Finessi, E., Mircea, M., Fuzzi, S., Moretti, F., Tagliavini, E., Ceburnis, D., and O’Dowd, C. D.: Important source of marine secondary organic aerosol from biogenic amines, *Environ. Sci. Technol.*, 42, 9116–9121, 2008.
- Franci, M. M., Pietro, W. J., Hehre, W. J., Binkley, J. S., Gordon, M. S., DeFrees, D. J., and Pople, J. A.: Self-consistent molecular orbital methods. XXIII. A polarization-type basis set for second-row elements, *J. Chem. Phys.*, 77, 3654–3665, 1982.
- Ge, X., Wexler, A. S., and Clegg, S. L.: Atmospheric amines – Part I. A review, *Atmos. Environ.*, 45, 524–546, 2011.
- Gibb, S. W., Mantoura, R. F. C., and Liss, P. S.: Ocean-atmosphere exchange and atmospheric speciation of ammonia and methylamines in the region of the NW Arabian Sea, *Global Biogeochem. Cy.*, 13, 161–178, 1999.
- Henschel, H., Navarro, J. C. A., Yli-Juuti, T., Kupiainen-Maatta, O., Olenius, T., Ortega, I. K., Clegg, S. L., Kurtén, T., Riipinen, I., and Vehkamäki, H.: Hydration of Atmospherically Relevant Molecular Clusters: Computational Chemistry and Classical Thermodynamics, *J. Phys. Chem. A*, 118, 2599–2611, 2014.
- Herb, J., Xu, Y., Yu, F., and Nadykto, A.: Large hydrogen-bonded pre-nucleation (HSO<sub>4</sub><sup>-</sup>)(H<sub>2</sub>SO<sub>4</sub>)<sub>m</sub>(H<sub>2</sub>O)<sub>k</sub> and (HSO<sub>4</sub><sup>-</sup>)(NH<sub>3</sub>)(H<sub>2</sub>SO<sub>4</sub>)<sub>m</sub>(H<sub>2</sub>O)<sub>k</sub> clusters in the Earth’s atmosphere, *J. Phys. Chem. A*, 117, 133–152, 2012.
- Huebert, B. J., Zhuang, L., Howell, S., Noone, K., and Noone, B.: Sulfate, nitrate, methanesulfonate, chloride, ammonium, and sodium measurements from ship, island, and aircraft during the Atlantic Stratocumulus Transition Experiment/Marine Aerosol Gas Exchange, *J. Geophys. Res.-Atmos.*, 101, 4413–4423, 1996.
- Kazil, J., Stier, P., Zhang, K., Quaas, J., Kinne, S., O’Donnell, D., Rast, S., Esch, M., Ferrachat, S., Lohmann, U., and Feichter, J.: Aerosol nucleation and its role for clouds and Earth’s radiative forcing in the aerosol-climate model ECHAM5-HAM, *Atmos. Chem. Phys.*, 10, 10733–10752, doi:<http://dx.doi.org/10.5194/acp-10-10733-2010>, 2010.
- 545 Kerminen, V., Aurela, M., Hillamo, R. E., and Virkkula, A.: Formation of particulate MSA: deductions from size distribution measurements in the Finnish Arctic, *Tellus B*, 49, 159–171, 1997.
- Kupiainen-Määttä, O., Olenius, T., Kurtén, T., and Vehkamäki, H.: CIMS sulfuric acid detection efficiency enhanced by amines due to higher dipole moments: a computational study, *J. Phys. Chem. A*, 117, 14109–14119, 2013.
- Leverentz, H. R., Siepmann, J. I., Truhlar, D. G., Loukonen, V., and Vehkamäki, H.: Energetics of atmospherically implicated clusters made of sulfuric acid, ammonia, and dimethyl amine, *J. Phys. Chem. A*, 117, 3819–3825, 2013.
- Loukonen, V., Kurtén, T., Ortega, I. K., Vehkamäki, H., Pádua, A. A. H., Sellegri, K., and Kulmala, M.: Enhancing effect of dimethylamine in sulfuric acid nucleation in the presence of water – a computational study, *Atmos. Chem. Phys.*, 10, 4961–4974, doi:<http://dx.doi.org/10.5194/acp-10-4961-2010>, 2010.

- 10-4961-201010.5194/acp-10-4961-2010, 2010.
- McGrath, M. J., Olenius, T., Ortega, I. K., Loukonen, V., Paa-  
sonen, P., Kurtén, T., Kulmala, M., and Vehkamäki, H.:  
Atmospheric Cluster Dynamics Code: a flexible method  
for solution of the birth-death equations, *Atmos. Chem.*  
*Phys.*, 12, 2345–2355, doi:http://dx.doi.org/10.5194/acp-12-  
2345-201210.5194/acp-12-2345-2012, 2012.
- Nadykto, A. B., Yu, F., Jakovleva, M. V., Herb, J., and Xu, Y.:  
Amines in the Earth's atmosphere: a density functional theory  
study of the thermochemistry of pre-nucleation clusters, *Entropy*,  
13, 554–569, 2011.
- Napari, I., Kulmala, M., and Vehkamäki, H.: Ternary nucleation of  
inorganic acids, ammonia, and water, *J. Chem. Phys.*, 117, 8418–  
8425, 2002.
- Olenius, T., Kupiainen-Määttä, O., Ortega, I., Kurtén, T., and  
Vehkamäki, H.: Free energy barrier in the growth of sulfuric  
acid–ammonia and sulfuric acid–dimethylamine clusters, *J.*  
*Chem. Phys.*, 139, 084312, doi:10.1063/1.4819024, 2013.
- Ortega, I. K., Kupiainen, O., Kurtén, T., Olenius, T., Wilk-  
man, O., McGrath, M. J., Loukonen, V., and Vehkamäki, H.:  
From quantum chemical formation free energies to  
evaporation rates, *Atmos. Chem. Phys.*, 12, 225–235,  
doi:http://dx.doi.org/10.5194/acp-12-225-201210.5194/acp-  
12-225-2012, 2012.
- Pierce, J. R. and Adams, P. J.: Uncertainty in global CCN  
concentrations from uncertain aerosol nucleation and pri-  
mary emission rates, *Atmos. Chem. Phys.*, 9, 1339–1356,  
doi:http://dx.doi.org/10.5194/acp-9-1339-200910.5194/acp-9-  
1339-2009, 2009.
- Solomon, S., Qin, D., Manning, M., Chen, Z., Marquis, M., Av-  
eryt, K. B., Tignor, M., and Miller, H. L.: IPCC, 2007: Cli-  
mate Change 2007: The Physical Science Basis. Contribution of  
Working Group I to the fourth assessment report of the Inter-  
governmental Panel on Climate Change, Cambridge University  
Press, Cambridge United Kingdom and New York, NY, USA,  
2007.
- Stewart, J. J.: Optimization of parameters for semiempirical meth-  
ods V: modification of NDDO approximations and application to  
70 elements, *J. Mol. Model.*, 13, 1173–1213, 2007.
- Van Dingenen, R. and Raes, F.: Ternary nucleation of methane sul-  
phonic acid, sulphuric acid and water vapour, *J. Aerosol Sci.*, 24,  
1–17, 1993.
- Weber, R., Marti, J., McMurtry, P., Eisele, F., Tanner, D., and Jef-  
ferson, A.: Measured atmospheric new particle formation rates:  
implications for nucleation mechanisms, *Chem. Eng. Commun.*,  
151, 53–64, 1996.
- Wyslouzil, B., Seinfeld, J., Flagan, R., and Okuyama, K.: Binary nu-  
cleation in acid–water systems. I. Methanesulfonic acid–water, *J.*  
*Chem. Phys.*, 94, 6827–6841, 1991.
- Zhao, Y. and Truhlar, D. G.: The M06 suite of density functionals  
for main group thermochemistry, thermochemical kinetics, non-  
covalent interactions, excited states, and transition elements: two  
new functionals and systematic testing of four M06-class func-  
tionals and 12 other functionals, *Theor. Chem. Acc.*, 120, 215–  
241, 2008.

**Table 1.** Comparison of various computational approaches for calculating Gibbs free binding energies. Unless otherwise stated, the basis set is 6-311++G(3df,3pd). F12 is shorthand for CCSD(T)-F12/VDZ-F12. Values in kcal mol<sup>−1</sup>.

Method	Gibbs free binding energy	
	H <sub>2</sub> SO <sub>4</sub> + DMA	MSA + DMA
M06-2X	−11.26	−7.42
B3LYP	−8.71	−4.59
PW91	−11.44	−7.75
ωB97X-D	−11.96	−8.98
MP2	−13.70	−10.84
F12//M06-2X	−11.72	−8.19
F12//B3LYP	−11.96	−8.57
F12//PW91	−12.07	−8.74
F12//ωB97X-D	−11.97	−9.33
F12//MP2	−11.99	−9.36
RI-MP2/AV(T+d)Z//		
RI-MP2/AV(D+d)Z	−12.49 <sup>1</sup>	−9.29 <sup>1</sup>
RI-MP2/AV(T+d)Z//		
BLYP/DZP	−15.57 <sup>2</sup>	
RI-CC2/AV(T+d)Z//		
B3LYP/CBSB7	−15.40 <sup>3</sup>	
PW91	−11.38 <sup>4</sup>	

References: <sup>1</sup> Dall'Osto et al. (2012), <sup>2</sup> Loukonen et al. (2010), <sup>3</sup> Ortega et al. (2012), <sup>4</sup> Nadykto et al. (2011).

**Table 2.** Testing the effect of CCSD(T)-F12/VDZ-F12 electronic energy corrections to M06-2X/6-311++G(3df,3pd) Gibbs free energy changes of the indicated reactions. Values in kcal mol<sup>−1</sup>.

Reaction	Gibbs free binding energy		
	F12//M06-2X	M06-2X	Δ <sub>F12-DFT</sub>
DMA + H <sub>2</sub> SO <sub>4</sub>	−11.72	−11.26	0.46
DMA + MSA	−8.19	−7.42	0.77
H <sub>2</sub> SO <sub>4</sub> + H <sub>2</sub> SO <sub>4</sub>	−7.07	−8.38	−1.31
H <sub>2</sub> SO <sub>4</sub> + MSA	−8.56	−10.70	−2.14
MSA + MSA	−7.53	−9.07	−1.54



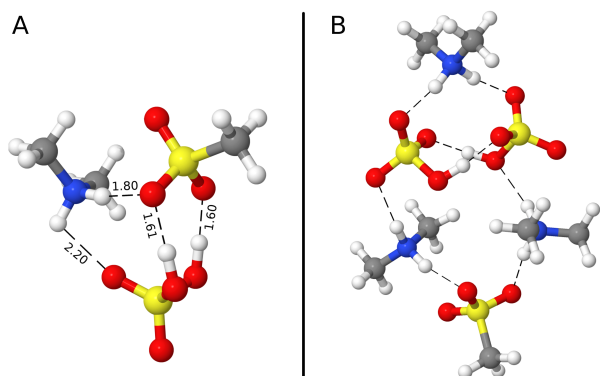


**Fig. 1.** (A) Most stable configuration of the MSA · H<sub>2</sub>SO<sub>4</sub> · DMA cluster. The lengths of the hydrogen bonds are given in Å. In this cluster, MSA is a stronger acid than H<sub>2</sub>SO<sub>4</sub>. (B) Configuration of the MSA · (H<sub>2</sub>SO<sub>4</sub>)<sub>2</sub> · DMA<sub>3</sub> cluster. As all investigated clusters, the most stable structure is more monolayer-like than bulk-like. The hydrogen bonds are shown as dashed lines.

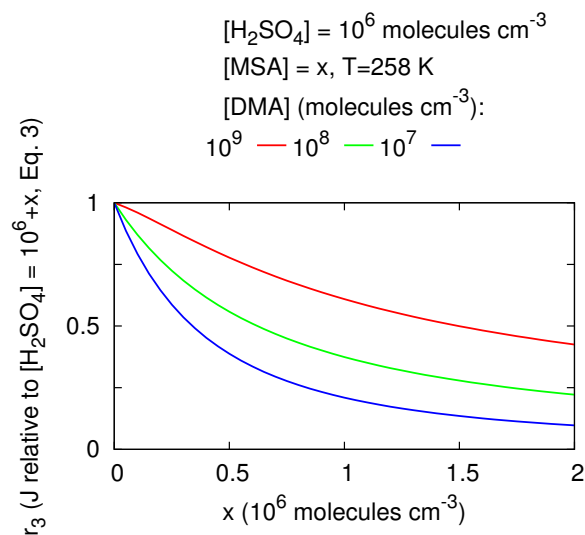


**Fig. 3.** Cluster formation rate of added MSA relative to the same amount of added H<sub>2</sub>SO<sub>4</sub> as defined in Eq. (3).

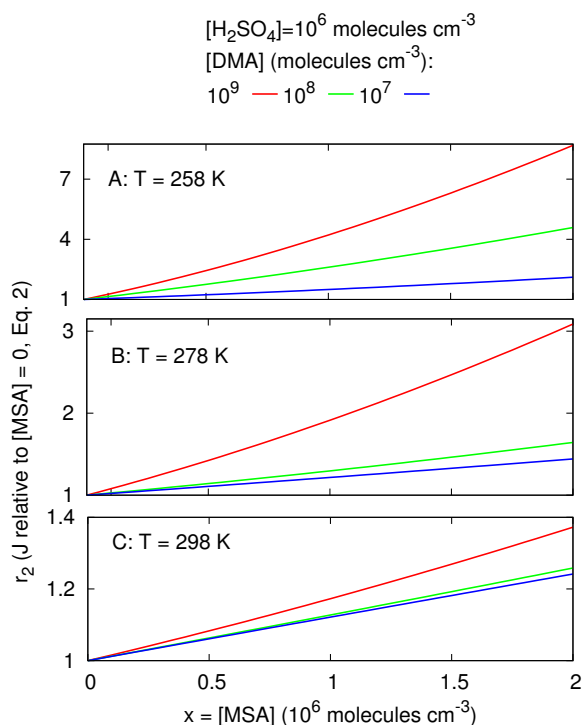


**Fig. 2.** MSA-H<sub>2</sub>SO<sub>4</sub>-DMA based particle formation rates at varying MSA concentrations relative to [MSA]=0 (Eq. 2).

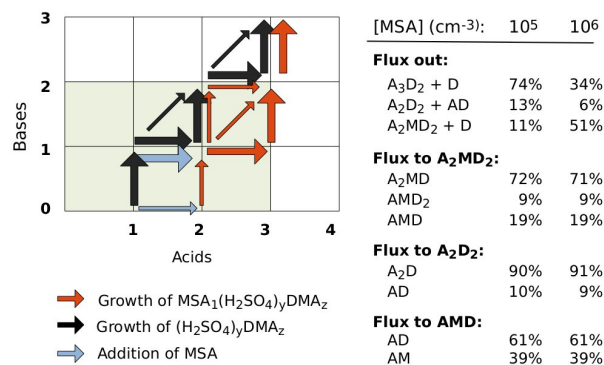


**Fig. 4.** Main cluster formation pathways at  $T = 258$  K and  $[\text{H}_2\text{SO}_4] = 10^6$  molecules  $\text{cm}^{-3}$ ,  $[\text{DMA}] = 10^8$  molecules  $\text{cm}^{-3}$  and two representative MSA concentrations. Dominating growth pathways are represented by thick arrows. Fluxes to clusters formed via several different pathways are indicated in the side table where A, M and D is shorthand for H<sub>2</sub>SO<sub>4</sub>, MSA and DMA, respectively.